Structure of Liquid Al_2O_3 from a Computer Simulation Model

Mahin Hemmati

Argonne National Laboratory, 9700 South Cass Avenue, Argonne, IL 60439

Mark Wilson* and Paul A. Madden

Physical and Theoretical Chemistry Laboratory, Oxford University, South Parks Road, Oxford OX1 3QZ, UK.

Received: August 26, 1998

The combination of new containerless sample and high intensity synchrotron source technologies has enabled the X-ray diffraction pattern from a molten oxide (Al_2O_3) to be determined for the first time (Ansell et al. *Phys. Rev. Lett.* **1997**, *78*, 464).[1] Here we show that the liquid-state diffraction pattern, predicted from a computer simulation with a potential derived from the ground-state crystal structure, agrees very well with the experimental data. Analysis of the local structure in the simulated melt shows that the Al^{3+} ions are not predominantly tetrahedrally coordinated, as surmised in the experimental study. Rather, six-, five- and four-coordinate Al^{3+} ions are found. Furthermore, evidence is presented for a tendency of the different coordinate species to spatially separate, and it is suggested that Al_2O_3 is close to a liquid−liquid phase separation of the type recently discussed by Angell and co-workers (*ACS Symp. Ser.* **1997**, *676*, 214).[2]

I. Introduction

Diffraction experiments offer a vital insight into the short (nearest-neighbor) and intermediate range structure of ionic systems in both the crystalline and liquid states.[3,4] However, the relatively high melting points of many ionic systems has precluded diffraction studies in the liquid state due to the problem of containing the sample. As a result, whole classes of important systems (notably the technologically interesting oxides and fluorides) have been out of range. Recent innovations[1] have shown that the need for a traditional sample container can be circumvented by the use of a levitated small sample droplet that is heated to the desired temperature with a laser. It has proven possible to record total X-ray structure factors of Al_2O_3 at two temperatures with such a sample by exploiting the well-collimated, high intensity X-rays from a synchrotron source. The study opens up a greatly widened range of systems for detailed microstructural investigation.

The purpose of the present article is to indicate how the information available from such studies can be greatly enhanced by combining the data with results from simulations with potentials that have been refined on crystalline-state information. Because of the experimental difficulties, only total structure factors $S(k)$ are available and the range of scattering vectors k is more limited than for more conventional studies. This means that there is some ambiguity in assigning the features of the radial distribution function, deduced by transformation of $S(k)$, to individual types of ion−ion correlations. By using a computer simulation that reproduces the experimental $S(k)$ well and *that has also been validated on other properties of the material of interest*, some of this ambiguity can be removed.

When an ionic compound melts, it is almost invariably found that the local coordination of the high-temperature crystal is preserved in the liquid state.[3,4] There are a number of exceptions, a well-known one being $AlCl_3$,[5] which melts from an ionic, six-coordinate crystal into a liquid in which the Al centers are four-coordinate. These tetrahedral centers share common edges to form neutral Al_2Cl_6 molecules so that the change in coordination number on melting is accompanied by an ionic to molecular transition. On the basis of the coordination numbers deduced from the diffraction study, it has been suggested that the Al centers in Al_2O_3 also undergo a drop in coordination number on melting. The lowest energy crystal structure is corundum, in which the Al^{3+} coordination number is 6 and the experimental study has shown a mean coordination number in the melt and glass of 4.5.

Such changes pose an interesting challenge for the interaction potentials used in computer simulations. Since the nature of the coordination environment varies strongly between the two phases, it can be imagined that the nature of the electronic properties of the ions themselves will also differ and hence that different interaction potentials would be required for each phase. Progress has been made, however, in developing potentials including the many-body effects that follow from the dependence of an ion's properties on its instantaneous coordination environment.[6] Such a potential has been shown to give a good representation of $AlCl_3$ in the liquid and solid phases, for example.[7] The simulation of Al_2O_3 presents a further specific problem; until recently it has not proven possible to find a potential that stabilizes the true ground-state crystal structure, corundum, relative to other polymorphs (notably bixbyite).[8] Recently, Wilson et al. developed a many-body Al_2O_3[9] potential that achieved this, and we will use a simplified version of this potential in the present work. On the basis of experience on other systems with a potential of this type, it would be expected to give a good description of the interactions in the liquid, as well as the solid, even allowing for the effects of possible changes in the local coordination on the effective interactions.

As we shall shortly see, simulations of the liquid with this potential do *not* show a predominance of four-coordinate Al ions, contrary to the experimental interpretation. Rather, the simulated liquid seems to consist of a mixture of six-, five-, and four-coordinate ions and the rate of exchange between six- and four-coordination seems fairly slow. More remarkably, the

10.1021/jp983529f CCC: $18.00
Published on Web 12/19/1998

TABLE 1: Potential Parameters for Al_2O_3[a]

	B_{ij}	α_{ij}	C_{ij}	b_{ij}
O−O	350.8837	2.41457	44.3729	1.44
Al−Al	0	0	0.216	
Al−O	63.4004	1.82657	2.1793	2.21

[a] All are in atomic units. The conversions for appropriate units are as follows: 1 au (energy) = $4.359\,748 \times 10^{-18}$ J; 1 au (length) = 0.529 177 Å; 1 au (time) = 2.4188×10^{-5} ps.

six- and four-coordinate ions seem to spatially separate within the liquid, which appears to be a precursor of the type of liquid−liquid phase separation that has been discussed in the context of deeply undercooled water[10] and other tetrahedral liquids.[11] There is experimental evidence to suggest that such a transition could occur in an Al_2O_3-like liquid. McMillan et al. reported the separation of two amorphous phases with the same chemical composition but different physical properties in an Al_2O_3/Y_2O_3 mixture.[12] Y^{3+} is an ion of somewhat larger radius than Al^{3+} and may promote the development of mixtures of coordination numbers in the melt.

II. Model

The solid-state potential for Al_2O_3 allows for the spherical "breathing"[13] of the oxide ions and for dipole and quadrupole polarization. The quadrupole polarization, whilst making a small contribution to the total energy (≃1%), plays an important role in stabilizing the experimentally observed crystal structure relative to other polymorphs. For the liquid-state studies, it has proven possible to simplify the potential by omission of the breathing and quadrupole polarization without significantly changing the predicted liquid-state structure. It would seem that the subtle structural consequences of these many-body effects, so important for the crystal structure, are washed out in this system by the high temperatures of the liquid-state studies and the fact that only averaged pair structures are measured.

The potential therefore used consists of dipole polarization terms plus a Born−Mayer pair potential to describe the short-range and dispersion interactions.

$$u(r_{ij}) = \frac{Q_i Q_j}{r_{ij}} + B_{ij} e^{-\alpha_{ij} r_{ij}} + \frac{C_{ij}}{r_{ij}^6} f_{ij}(r) \qquad (1)$$

The parameters are given in Table 1. The experimental refractive index in the crystalline corundum ground state, coupled with an ab initio cation polarizability of 0.265 au,[14] gives an oxide ion polarizability of 9.23 au.[9,15] The dipole−dipole dispersion coefficients, C_{ij}, are derived from these polarizabilities via the Slater−Kirkwood formula (as in ref 9) and are given in Table 1. The effects of dispersion damping (the change of dispersion interaction energy due to overlap away from the asymptotic value) are included via a Tang−Toennies function,[16] $f_{ij}(r)$. The *b* parameters associated with this function are also given in Table 1. The repulsive part of the pair potential is the same as that used by Grimes et al.[17] Anion polarization effects are included to a dipolar level via a polarizable-ion model[9,18,19] with the anion polarizability of 9.23 au. A short-range damping parameter of 1.65 au is used so that the dipole polarization terms are as in the study of crystalline Al_2O_3.[9,20]

Periodic boundary conditions were applied with the long-range coulomb forces treated via an Ewald summation. Nose-Hoover thermostats were employed to control both the ion translational motions and the "fake" dipolar motion. Simulations were performed in the canonical ensemble (NVT) at a density of 3.97 g/cm^3 taken from ref 1, with a total number of 640 ions. The system was melted at a temperature of 5000 K, allowed to run for 50 ps at this temperature, and then cooled to the temperature of the experimental study (2663 K). An equilibration run of over 100 ps was then performed with a subsequent production run of 50 ps. The pressure fluctuated about zero throughout.

III. Liquid Structure: Comparison of Experiment and Simulation

A. Structure Factors. Partial structure factors are calculated directly from

$$S_{\alpha\beta}(k) = \frac{1}{\sqrt{N_\alpha N_\beta}} \left\langle \sum_{i=1}^{N_\alpha} e^{ikr^i} \sum_{j=1}^{N_\beta} e^{-ikr^j} \right\rangle \qquad (2)$$

where N_α is the number of ions of type α, for *k* values up to 2.3 Å^{-1} in order to circumvent the effect of truncation errors in a Fourier transformation of a radial distribution function. For higher *k* values, the partials are obtained by Fourier transforming the partial radial distribution functions.

The total X-ray weighted structure factor, $S_X(k)$, is calculated by adding the three partial structure factors with the X-ray form factors, $f(k)$, and the concentration factors, *c*.

$$S_X(k) = \frac{f_+^2 c_+ S_{++} + 2 f_- f_+ \sqrt{c_- c_+} S_{+-} + f_-^2 c_- S_{--}}{f_+^2 c_+ + f_-^2 c_-} \qquad (3)$$

The Al^{3+} form factor may be taken from standard tables,[21] but the form factor for O^{2-} presents a special problem, because the O^{2-} ion is unstable in the gas phase. We have used the form factor given in reference,[22] which is obtained from electronic structure calculations on an O^{2-} ion in a Watson-sphere environmental potential. Form factors are usually quoted as

$$f(k) = \sum_{i=1}^{4} a_i \exp[-b_i (k/4\pi)^2] + c \qquad (4)$$

and the parameters are given in Table 2.

Figure 1 shows the partial structure factors weighted with the appropriate form and concentration factors along with the total structure factor. The calculation shows that, because of the particular weightings of the different partials, the shape of the total structure factor involves subtle cancelations and is not simply related to a single partial at any value of *k*. In particular, the principal peaks in the Al−Al and O−O partials are very strongly cancelled by the Al−O contribution so that the first distinctive feature in the total structure factor at ∼2.1 Å^{-1}, called a "prepeak" in the experimental paper,[1] arises because the low-*k* parts of all three partials are in phase and is not associated with a peak in any partial. The strong peak at ∼4.5 Å^{-1} is associated with the second peak in the Al−Al partial.

Comparison of the calculated and experimental structure factors is complicated by the presence of an air scattering contribution, due to the difficulty of performing a scattering experiment on a levitated droplet, which becomes important for low *k*.[1] Excellent agreement is obtained for $k > 3$ Å^{-1}, and at lower *k*, it would also be achieved if a (roughly) exponentially decaying component, representing the air contribution, were to be removed from the experimental data. It is already clear however that the shape, position, and amplitude of the simulation "prepeak" closely resemble the experimental one.

B. Real Space Structure: Decomposition into Partials. We may also compare a total X-ray weighted radial distribution

TABLE 2: Form Factors

	a_1	b_1	a_2	b_2	a_3	b_3	a_4	b_4	c
Al^{3+} (ref 21)	4.174 48	1.938 16	3.387 60	4.145 53	1.202 96	0.228 753	0.528 137	8.285 24	0.706 786
O^{-2} (ref 22)	4.758	7.831	3.637	30.05	0	0	0	0	1.594

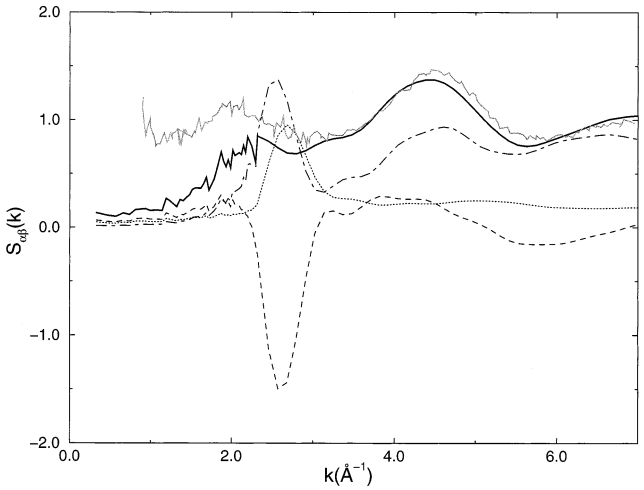

Figure 1. Partial and total structure factors for liquid Al_2O_3 at 2663 K: (dotted line) $S_{OO}(k)$; (dashed line) $S_{AlO}(k)$; (dot-dashed line) $S_{AlAl}(k)$; (full lines) total structure factors; the dark and light lines are the simulated and experimental structure factors, respectively.

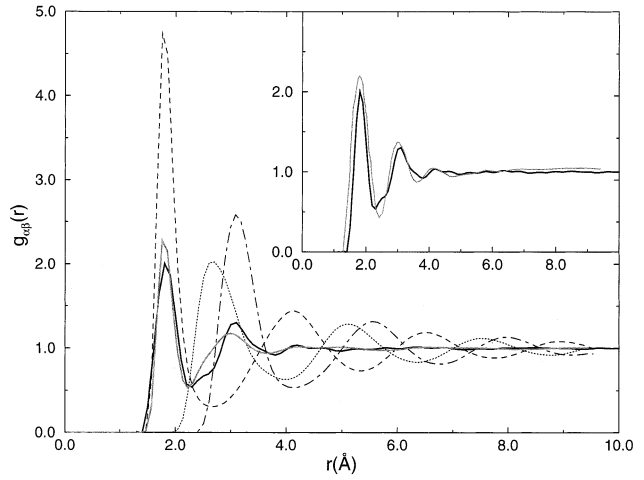

Figure 2. Partial radial distributions for liquid Al_2O_3 at 2663 K: (dotted line) $g_{OO}(r)$; (dashed line) $g_{AlO}(r)$; (dot-dashed line) $g_{AlAl}(r)$; (full lines) the calculated total X-ray rdfs $g_X(r)$ (dark line) and $\tilde{g}_X(r)$ (light line). The inset to the figure shows the comparison of $g_X(r)$ with the experimental rdf.

function (rdf), $g_X(r)$, obtained by inverse transforming the calculated X-ray structure factor at 2663 K, with that quoted in the experimental paper. This is shown in the inset to Figure 2; it reveals good accord in the information about the real space structure that may be deduced from experiment. The positions and amplitudes of the major features agree well; the simulated peaks are somewhat narrower, which may be associated with the range of k values included in the fourier transformation.

The figure also shows the relationship between the X-ray rdf and the partial rdfs. Notable features are the persistence out to long range of the oscillations in the partials. These oscillations and their phase relationship are typical of a system where the intermediate and long-range structure is charge ordered. Because of the weighting of the different partials, little evidence of these oscillations persists in the total rdf. The partial rdfs also show that the system is a "charge-ordered" ionic system at shorter range in that the first peak in $g_{AlAl}(r)$ occurs at greater separations than that in $g_{OO}(r)$, reflecting the greater coulombic repulsion between a pair of triply charges aluminium ions. This is in contrast to systems such as $ZnCl_2$ or $BeCl_2$ in which large anion polarization effects act to screen the cation−cation interactions and allows pairs of cations to approach closely.[6]

The figure demonstrates clearly the problems inherent in interpreting the experimental *total* rdf in a multicomponent system such as that considered here. In ref 1, the first peak in $g_X(r)$ is interpreted as arising predominantly from $g_{AlO}(r)$ and the second from $g_{OO}(r)$. Figure 2 shows that, for the simulated fluid, the first assignment is reasonable whilst that for the second peak is largely incorrect; in fact, the second peak arises from a superposition of $g_{OO}(r)$ and $g_{AlAl}(r)$, resulting in a peak position approximately intermediate between the peaks in the two partial rdfs. Additionally, the further experimental assignment of the peak at ∼4.25 Å to the next-nearest neighbor O−O interactions appears erroneous. The origin of this peak in the simulated function arises from an incomplete cancelation between the second peak in $g_{AlO}(r)$ with the first troughs in $g_{OO}(r)$ and $g_{AlAl}(r)$.

These problems are associated with the significance of peak *positions*. A second source of difficulty concerns the *intensity* of the peaks in the X-ray weighted rdf. In the figure, the X-ray weighted rdf, $g_X(r)$ is compared with the superposition of partial rdfs weighted by the $k = 0$ values of the form factors, $\tilde{g}_X(r)$, which would be the X-ray rdf if the atoms behaved as point scattering centers and the k dependence of the form factors was negligible. This shows that the k dependence of the O^{2-} form factor has a significant affect on the real space structure—the height of the first peak is reduced, and the position and width of the second peak are shifted (since this is made up of a superposition of two partials). Despite the fact that the first peak of $g_X(r)$ arises from $g_{AlO}(r)$, it is therefore difficult to reliably determine the coordination number of the Al^{3+} ions simply by integrating over the first peak of $g_X(r)$.

IV. Analysis of the Structure of the Simulated Fluid

A. Coordination Numbers. Coordination numbers were assigned to the Al^{3+} ions by counting the number of oxide ions within a sphere of radius equal to the position of the first minimum (2.6 Å^{-1}) in g_{AlO}. Figure 3 shows the distribution of coordination numbers calculated over the length of the run. These indicate a range of aluminium coordination numbers from 4 to 6 in the ratios 27.1%, 52.7%, and 20.2% for four-, five-, and six-coordinate Al^{3+}, respectively.

Figure 4 shows the Al−O−Al and O−Al−O bond angle distributions calculated using the first minimum in the Al−O partial rdf as the cutoff. The O−Al−O distribution shows a peak at around 85° with a shoulder at 110° characteristic of the distribution of tetrahedra and octahedra hinted at by Figure 3. The Al−O−Al distribution shows a main peak at ≃100° with a shoulder at ≃120°. The main peak is characteristic of edge-sharing octahedral units with the latter, more open angle characteristic of single bridges between lower-coordinate Al^{3+} species. To the extent that it is useful to compare the local structure in a high-temperature liquid to a crystal structure, that of Al_2O_3 appears most closely related to either θ-Al_2O_3 ($\equiv\beta$-Ga_2O_3) or the spinel Al_2O_3, both of which have a mixture of cations in tetrahedral and octahedral sites in essentially close-packed anion sublattices.

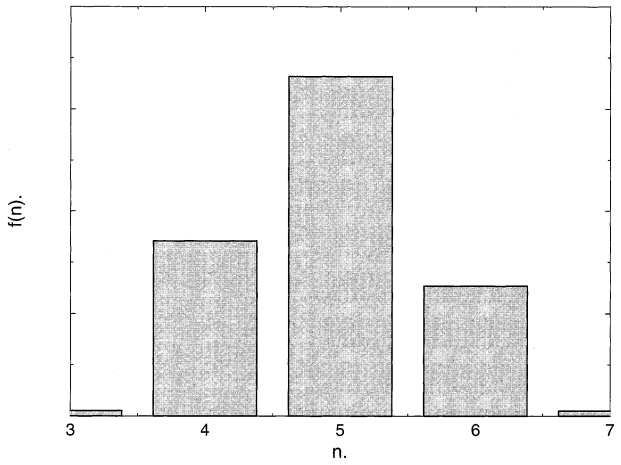

Figure 3. Coordination number distribution about the Al^{3+} cations for liquid Al_2O_3 at 2663 K.

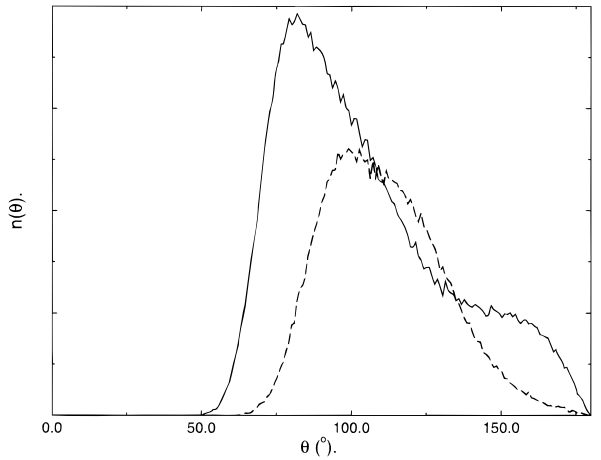

Figure 4. Bond angle distributions for liquid Al_2O_3 at 2663 K: (full line) O−Al−O; (dashed line) Al−O−AI.

The finding of appreciable numbers of five- and six-coordinated Al^{3+} ions in the simulated melt does not accord well with the interpretation of the experimental data,[1] where a mean coordination number close to 4 is reported and a tetrahedral network structure is proposed on the basis of the relationship between the positions of the second and third peaks in $g_X(r)$. However, as we have seen, the deduction of a mean coordination number from the integral of the first peak in $g_X(r)$ is made difficult by the role of the O^{2-} form factor. From Figure 2 (inset), it would appear that a coordination number deduced in this way from the simulated $g_X(r)$ would be *lower* than that for the experimental data. Further, the third peak in $g_X(r)$ does not correspond to a peak in any of the partial rdfs.

Additional information about the normal coordination environment about the Al^{3+} cations comes from ^{27}Al NMR experiments.[23−26] In both the glassy Al_2O_3/SiO_2 and Al_2O_3/CaO systems with a high alumina content, coordination numbers about the Al^{3+} ion from 4 to 6 are observed with the relative amounts governed by the glass quench rate (the faster the quench the greater the number of five-coordinate sites).[25,26]

B. Al−O "Bondlength" in Different Coordination Environments. We can highlight an experimentally observable consequence of the range of coordination environments by returning to the partial radial distribution functions. Figure 5a shows the partial rdfs for the Al_2O_3 liquid at 2663 K compared with those for SiO_2 at 3000 K. SiO_2 has a much sharper distribution of cation coordination environments centered about

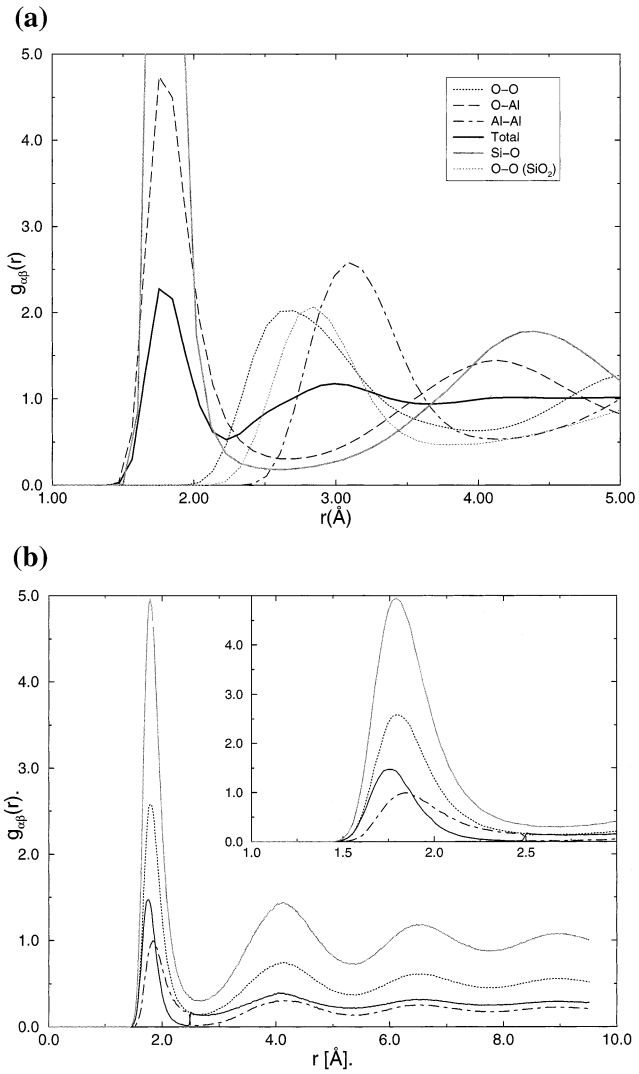

Figure 5. Comparison of the radial distribution functions (a) with those for SiO_2: (black dotted line) $g_{OO}(r)$ in Al_2O_3; (dashed line) $g_{AlO}(r)$, (dot-dashed line) $g_{AlAl}(r)$; (light dotted line) $g_{OO}(r)$ in SiO_2; (light full line) $g_{SiO}(r)$. (b) $g_{AlO}(r)$ for specific Al^{3+} coordination environments: (full line) $Al^{3+}_{[4]}-O^{2-}$; (dotted line) $Al^{3+}_{[5]}-O^{2-}$; (dot-dashed line) $Al^{3+}_{[6]}-O^{2-}$; (light full line) total. The inset shows the first peak in detail.

4[27] (with around 75% of the cations four-coordinate). The Si−O and O−O curves for SiO_2 have been scaled by the relative positions of the first peaks in g_{AlO} and g_{SiO}. It is clear that g_{SiO} is significantly sharper than g_{AlO} having a full width half maximum of 0.2 Å, compared with 0.4 Å. Similarly, g_{OO} in SiO_2 is significantly sharper than that in Al_2O_3, with a scaled first peak position at longer range. These factors point to the larger range of coordination environments in Al_2O_3, which contribute to both g_{AlO} and g_{OO} on differing length scales resulting in broader peaks.

Al^{3+} coordination-number-specific pair rdfs can be defined between ion pairs of specific types

$$4\pi r^2 g_{\alpha\beta}(r) = \frac{V}{\sqrt{N_\alpha N_\beta}} \sum_{i=1}^{N_\alpha} \sum_{j=1}^{N_\beta} \delta(|\mathbf{r}_i - \mathbf{r}_j| - r) \qquad (5)$$

where $\{\alpha, \beta\}$ may label the instantaneous coordination number of an Al^{3+} ion as calculated above. Here, we consider the distributions between the four-, five-, and six-coordinate Al^{3+}

ions and the oxide ions ($g_{Al_{[4]}O}$, $g_{Al_{[5]}O}$ and $g_{Al_{[6]}O}$). Figure 5b shows these pair distribution functions normalized for the total number of $Al^{3+}-O^{2-}$ pairs. As expected from Figure 3, the five-coordinate sites contribute most to the total pair distribution function. The respective peak positions are 1.76, 1.80, and 1.86 Å for $Al^{3+}_{[4]}$, $Al^{3+}_{[5]}$, and $Al^{3+}_{[6]}$, reflecting the expected reduction in anion−cation bond length with decreasing coordination number. Indeed, the change in bond length of around 5% from the six- to four-coordinate environment is typical of the alkaline earth oxides[28] and SiO_2.[29] These values are consistent with those derived from ^{27}Al NMR experiments.[25,26]

It is interesting to note that the six-coordinate bond length of 1.86 Å is equivalent to the *shortest* bond length in the six-coordinate corundum crystal structure (in which the Al^{3+} ion sits in a distorted octahedral hole resulting in an effective 3 + 3 coordination with bond lengths of 1.86 and 1.97 Å). Again, this is not surprising as the bond lengths in the crystal are affected by the higher symmetry of the sites leading to a greater influence for other ion−ion interactions (for example, the $Al^{3+}-Al^{3+}$ in corundum[9]). Thus, even for the six-coordinate ions, the mean nearest-neighbor separation contracts on melting. This is the normal finding in the melting of ionic materials, including those in which the coordination number is preserved on melting.[5] Such a contraction is not necessarily indicative of a reduction in coordination number.

Another feature of interest in the $g_{Al_{[n]}O}$s is the depth of the first minimum in the different functions. It is seen that in $g_{Al_{[4]}O}$ the first minimum is almost at zero, whereas in $g_{Al_{[5]}O}$ and $g_{Al_{[6]}O}$ the minimum value is considerably greater. The picture that emerges is of a tightly coordinated AlO_4 unit, with only slow exchange of O^{2-} ions between the coordination shell and the bulk, whereas in the five- and six-coordinated species, the O^{2-} ions are less tightly held and may exchange relatively freely. Other measures (such as simply counting the number of changes in the coordination number) indicate that the five- and six-coordinate species interchange fairly freely whereas exchange between four- and five-coordination is slow. It is tempting to speculate that there are two basic "species" of Al^{3+} present, the four- and six-coordinate ones, with the five-coordinate arising as a strongly distorted version of the six-coordinate.

C. "Phase" Separation of the Differently Coordinated Ions? The analogy between the local liquid structure and that of crystals raises the issue of how differently coordinated cations are mutually arranged in the liquid phase. In the crystal structures mentioned above, the four- and six-coordinate ions occupy interpenetrating lattices. On the other hand, one can envisage the possibility that the high- and low-coordination species might tend to cluster. Recently, a similar phenomenon in supercooled water[10] has been highlighted and has lead to the hypothesis that a liquid−liquid phase separation can occur in which the resulting liquid phases differ only in density and not in composition. A direct observation of phase separation of droplets of apparently identical composition to the surrounding matrix in a glassy Y_2O_3/Al_2O_3 mixture has been reported.[12]

Figure 6 shows a molecular dynamics "snapshot" of the liquid Al_2O_3 at 2663 K in which bonds have only been drawn between $Al^{3+}_{[6]}-O^{2-}$ pairs. It is clear that the six-coordinate Al^{3+} cations are grouped together in this instantaneous configuration. A statistically averaged measure of this tendency is best obtained by calculation of the partial structure factors of the differently coordinated Al^{3+} centers (averaged over the simulation run). Figure 7 shows the partial Al−Al structure factors for the like-coordination environments. The $Al^{3+}_{[6]}-Al^{3+}_{[6]}$ function shows a

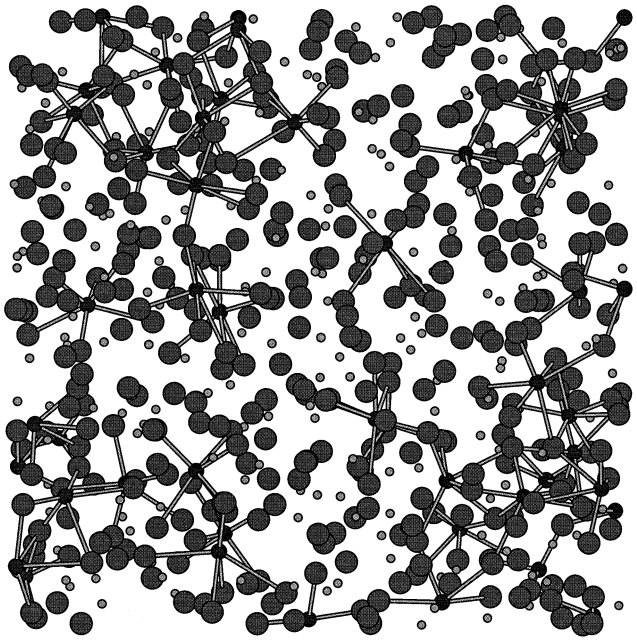

Figure 6. Molecular graphics "snapshot" highlighting the six-coordinate Al^{3+} ions. The largest circles represent the anion coordinates; the smallest ions are the non-six-coordinate aluminiums, with the intermediate sized circles being the six-coordinate ions. Bonds are only drawn between Al−O pairs for six-coordinate cations. Some cations may appear to have a coordination number less than 6 due to the effect of boundary conditions.

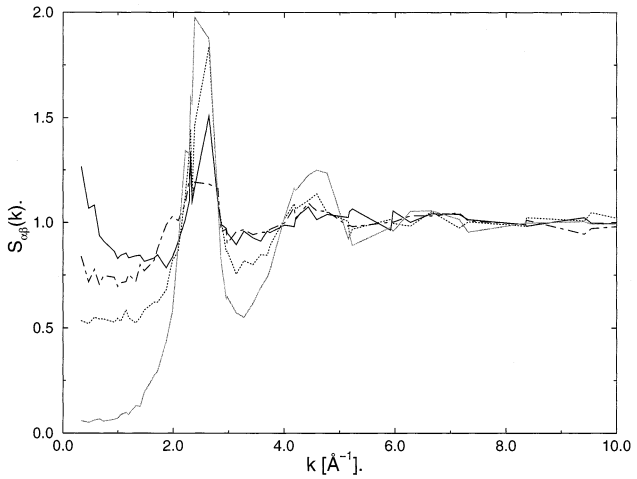

Figure 7. Partial structure factors for specific Al^{3+} coordination environments: (dot-dashed line) $Al^{3+}_{[4]}-Al^{3+}_{[4]}$; (dotted line) $Al^{3+}_{[5]}-Al^{3+}_{[5]}$; (full line) $Al^{3+}_{[6]}-Al^{3+}_{[6]}$; (light full line) all $Al^{3+}-Al^{3+}$.

clear rise in intensity as $k \rightarrow 0$ indicative of a clustering tendency of the six-coordinate species. Similar observations have been reported in supercooled water.[10]

The origin of the clustering tendency appears to be the nature of the linkages that must be formed between the different coordination centers in order to preserve stoichiometry and charge neutrality on intermediate and long length scales. If an Al^{3+} ion is to have five or six nearest neighbors in a system of stoichiometry Al_2O_3, it implies that there must be a high degree of sharing of the O^{2-} "ligands" involving several Al^{3+} ions. The snapshot shown in Figure 6 indicates that the five- and six-coordinate Al^{3+} ions are adept at binding O^{2-} through edge-sharing between their coordination polyhedra.

The clear implication of this finding is that liquid Al_2O_3 (certainly this simulation model of it) may be in the vicinity of

a critical point below which liquid−liquid phase separation will occur.

V. Summary

The potential used in the present work is a simplified version of one that correctly predicts the ground-state crystal structure of Al_2O_3. In the crystal, many-body "breathing" and quadrupole polarization effects help to tip the relative stability of the lowest energy crystal towards corundum relative to other structures. However, these effects seem to have little effect on the average pair structure of the high-temperature liquid, although the dipole polarization does come into play, owing to the low symmetry of the instantaneous coordination environments of O^{2-}.

The simulated X-ray structure factor is in good agreement with experiment. Analysis of the contribution of the partials to this total structure factor (and the attendant total rdf) highlights some of the difficulties involved in deducing the atomic structure directly from this data. The peaks in these functions do not, in general, correspond to peaks in the partials, making the assignment of the interatomic separations difficult. Furthermore, the nontrivial k dependence of the O^{2-} form factor affects the coordination numbers deduced from integrals over peaks in the X-ray rdf.

The simulated fluid shows a tendency for spatial separation of the six- and four-coordinate Al^{3+} ions and appears to be on the verge of separating into two fluid phases with the same chemical composition. It would appear that Al_2O_3 is a good candidate for studying the phenomenon of polyamorphism in the liquid state, as proposed by Poole et al.[10]

Acknowledgment. M.W. thanks the Royal Society for a fellowship. The work was supported by EPSRC Grant GR/L/49369.

References and Notes

(1) Ansell, S.; Krishnan, S.; Weber, J. K. R.; Felten, J. J.; Nordine, P. C.; Beno, M. A.; Price, D. L.; Saboungi, M. L. *Phys. Rev. Lett*. **1997**, *78*, 464.

(2) Yarger, J. L.; Angell, C. A.; Borick, S. S.; Wolf, G. H. *ACS Symp. Ser.* **1997**, *676*, 214.

(3) Rovere, M.; Tosi, M. P. *Rep. Prog. Phys.* **1986**, *49*, 1001.

(4) Enderby, J. E.; Barnes, A. C. *Reps. Prog. Phys.* **1990**, *53*, 85.

(5) Pastore, G.; Tatlipinar, H.; Tosi, M. P *Phys. Chem. Liq.* **1996**, *31*, 189. Akdeniz, Z.; Pastore, G.; Tosi, M. P. *Phys. Chem. Liq.* **1996**, *32*, 191.

(6) Madden, P. A.; Wilson, M. *Chem. Soc. Rev.* **1996**, *25*, 339.

(7) Walters, M. K.; Hutchinson, F.; Rowley, A. J.; Madden, P. A. In preparation.

(8) Gale, J. D.; Catlow, C. R. A.; Mackrodt, W. C. *Modell. Simul. Mater. Sci. Eng*. **1992**, *73*, 1.

(9) Wilson, M.; Exner, M.; Huang, Y.; Finnis, M. W. *Phys. Rev. B* **1996**, *54*, 15683.

(10) Harrington, S.; Zhang, R.; Poole, P. H.; Sciortino, F.; Stanley, H. E. *Phys. Rev. Lett.* **1997**, *78*, 2409.

(11) Poole, P. H.; Grande, T.; Angell, C. A.; McMillan, P. F. *Science* **1997**, *275*, 322.

(12) Aasland, S.; McMillan, P. F. *Nature* **1994**, *369*, 633.

(13) Wilson, M.; Madden, P. A.; Pyper, N. C.; Harding, J. H. *J. Chem. Phys*. **1996**, *104*, 8068.

(14) Pyper, N. C. *Adv. Sol. Stat. Chem.* **1991**, *2*, 223.

(15) Gitzen, W. H. *Alumina as a Ceramic Material*; The American Ceramic Society: Columbus, OH, 1970.

(16) Tang, K. T; Toennies, J. P. *J. Chem. Phys.* **1984**, *80*, 3726.

(17) Grimes, A. W. *J. Am. Ceram. Soc*. **1994**, *77*, 378.

(18) Wilson, M.; Madden, P. A. *Faraday Discuss*. **1997**, *105*, 1.

(19) Wilson, M.; Madden, P. A.; Costa-Cabral, B. J. *J. Phys. Chem*. **1996**, *100*, 1227.

(20) Wilson, M. *J. Am. Ceram. Soc.*, to be published.

(21) Cromer, D. T.; Waber, J. T. *International Tables for X-Ray Crystallography*; Ibers, J. A., Hamilton, W. C., Eds.; Kynoch Press: Birmingham, 1974; p 71.

(22) Tokonami, M. *Acta Crystallogr*. **1965**, *19*, 486.

(23) Coutures, J. P.; Massiot, D.; Bessada, C.; Echegut, P.; Rifflet, J. C.; Taulette, F.; *C. R. Acad. Sci.* **1990**, *310*, 1041.

(24) Massiot, D.; Taulette, F.; Coutures, J. P. *Colloq. Phys.* **1990**, *C5*, 425.

(25) Sato, R. K.; McMillan, P. F.; Dennison, P.; Dupree, R. *J. Phys. Chem.* **1991**, *95*, 4483.

(26) Poe, B. T.; McMillan, P. F.; Cote, B.; Massiot, D.; Coutures, J. P. *J. Phys. Chem.* **1992**, *96*, 8220.

(27) Hemmati, M.; Angell, C. A. *J. Non-cryst. Solids* **1997**, *217*, 236.

(28) Wilson, M.; Madden, P. A. *Mol. Phys.* **1997**, *90*, 75.

(29) Meade, C.; Hemley, R. J.; Mao, H. K. *Phys. Rev. Lett.* **1992**, *69*, 1387.